

Higgs-radion interpretation of the LHC Higgs hints

John F. Gunion¹

¹Department of Physics, U.C. Davis, Davis CA 95616, USA

DOI: will be assigned

Higgs-Radion interpretation of the LHC data?

We explore a Higgs-radion interpretation of the LHC Higgs-like excesses seen by ATLAS and CMS in the current data set.

1 Introduction

The two simplest ways of reconciling the weak energy scale $\mathcal{O}(1 \text{ TeV})$ and the much higher GUT or reduced Planck mass scale $m_{Pl} \sim \mathcal{O}(10^{18} \text{ GeV})$ in a consistent theory are (i) to employ supersymmetry or (ii) to introduce one or more warped extra dimensions. In this contribution, I summarize the results of [1] in which we pursue the 5D version of the latter introduced by Randall and Sundrum (RS) [2], but modified in that all fields other than the Higgs reside in the bulk. Having the gauge and fermion fields in the bulk is needed to adequately suppress flavor changing neutral current (FCNC) operators and to keep corrections to precision electroweak (PEW) observables small [3, 4, 5, 6, 7, 8, 9, 10].

By placing the Higgs field on the TeV brane its vev can naturally be order a TeV vs m_{Pl} as a result of the RS metric “warp factor” $\Omega_0 \equiv e^{-m_0 b_0/2}$: $v_0 = \Omega_0 m_{Pl} \lesssim 1 \text{ TeV}$ for $m_0 b_0/2 \sim 35$. (Our notation will basically follow that of [11].) This is a great improvement compared to the original problem of accommodating both the weak and the Planck scale within a single theory.

The quantum excitations of the gravitational metric are the Kaluza-Klein (KK) modes $h_{\mu\nu}^n(x)$ (with mass m_n) and the quantum excitation associated with the distance between the two branes is the radion field $\phi_0(x)$. The vacuum expectation value of the radion field is denoted by Λ_ϕ which is related to the Planck mass by $\Lambda_\phi = \sqrt{6}\Omega_0 m_{Pl}$. To solve the hierarchy problem, Λ_ϕ should be no larger than 10 TeV, with $\Lambda_\phi \sim 1 - 3 \text{ TeV}$ preferred. In addition to the radion, the model contains a conventional Higgs boson, h_0 .

The ratio m_0/m_{Pl} is a particularly crucial parameter that characterizes the 5-dimensional curvature. As discussed shortly, large curvature values $m_0/m_{Pl} \gtrsim 0.5$ are favored for fitting the LHC Higgs excesses and by bounds on FCNC and PEW constraints. In early discussions of the RS model it was argued that $R_5/M_5^2 < 1$ (M_5 being the 5D Planck scale and $R_5 = 20m_0^2$ the size of the 5D curvature) is needed to suppress higher curvature terms in the 5D action, which leads to $m_0/m_{Pl} \lesssim 0.15$ being preferred. However [10] argues that R_5/Λ^2 (with Λ being the energy scale at which the 5D gravity theory becomes strongly coupled, estimated by naive dimensional analysis to be $\Lambda \sim 2\sqrt{3}\pi M_5$) is the appropriate measure, implying that values as large as $m_0/m_{Pl} < \sqrt{3\pi^3/(5\sqrt{5})} \sim 3$ are acceptable.

Let us comment on how it is that propagation of the gauge and matter fields in the bulk can ameliorate the FCNC and PEW problems. In this case, the SM particles are the zero-modes of the 5D fields and the profile of a SM fermion in the extra dimension can be adjusted using a mass parameter. If 1st and 2nd generation fermion profiles peak near the Planck brane then FCNC operators and PEW corrections will be suppressed by scales $\gg \text{TeV}$. Even with this arrangement it is estimated that the masses of the first KK excitations g^1 , W^1 and Z^1 must be larger than about 3 TeV (see the summary in [10]). Another more direct bound on the g^1 mass comes from collider experiments. First, there is a universal component to the light quark coupling $q\bar{q}g^1$ that is roughly equal to the SM coupling g times a factor of ζ^{-1} , where $\zeta \sim \sqrt{\frac{1}{2}m_0 b_0} \sim 5 - 6$. The suppression is due to the fact that the light quarks are localized near the Planck brane whereas the KK gluon is localized near the TeV brane. Even with such suppression, the LHC g^1 production rate due to $u\bar{u}$ and $d\bar{d}$ collisions is large. Further, the $t_R\bar{t}_R g^1$ coupling is large since the t_R profile peaks near the TeV brane – the prediction of [12] is $g_{t_R\bar{t}_R g^1} \sim \zeta g$. As a result, the dominant decay of the

g^1 is to $t\bar{t}$. ATLAS and CMS search for $t\bar{t}$ resonances at high mass. Using $g_{q\bar{q}g^1} \sim g/5$, $q = u, d$, one finds a lower bound of $m_1^g \gtrsim 1.5$ TeV [13] using an update of the analysis of [12]. ([14] gives a weaker bound of $m_1^g > 0.84$ TeV.) .

In terms of Λ_ϕ , we have the following relations:

$$\frac{m_0}{m_{Pl}} = \frac{\sqrt{6} m_1^g}{x_1^g \Lambda_\phi} \simeq \frac{m_1^g}{\Lambda_\phi}, \quad \text{and} \quad \frac{1}{2} m_0 b_0 = -\log \left(\frac{\Lambda_\phi}{\sqrt{6} m_{Pl}} \right) \quad (1)$$

where $x_1^g = 2.45$ is the 1st zero of an appropriate Bessel function. If the model really solves the hierarchy problem then Λ_ϕ cannot be much larger than 1 TeV and certainly $\Lambda_\phi \leq 10$ TeV. If we adopt the CMS limit of $m_1^g > 1.5$ TeV then Eq. (1) implies a lower limit on the 5-dimensional curvature of $m_0/m_{Pl} \gtrsim 0.15$. Thus, a significant lower bound on m_1^g implies that only relatively large values for m_0/m_{Pl} are allowed. As discussed above, m_0/m_{Pl} values up to $\sim 2 - 3$ are probably consistent with curvature corrections to the RS scenario being small. Still, tension between the lower bound on m_1^g and keeping acceptably small m_0/m_{Pl} could increase to an unacceptable point as the LHC data set increases. We will discuss the phenomenology that applies if the value of Λ_ϕ for any given (m_0/m_{Pl}) is tied to the lower bound of $m_1^g = 1.5$ TeV using Eq. (1). Alterations to the phenomenology using $m_1^g = 3$ TeV, as perhaps preferred by PEW constraints, will also be illustrated.

However, as described in [1], there are alternative approaches in which the tie between m_1^g and Λ_ϕ of Eq. (1) is not present or is very uncertain. In this case, it becomes appropriate to discuss the phenomenology that arises for fixed Λ_ϕ as m_0/m_{Pl} is varied. This will be discussed for $\Lambda_\phi = 1$ TeV and 1.5 TeV.

Since the radion and Higgs fields have the same quantum numbers, it is generically possible to introduce mixing between them. The mixing action [15] has magnitude dictated by a coefficient parameter ξ . The physical mass eigenstates, h and ϕ , are obtained by diagonalizing and canonically normalizing the kinetic (and mass) terms in the Higgs-radion Lagrangian. The diagonalization procedures and results for the h and ϕ using our notation can be found in [11] (see also [15, 16]). The resulting Feynman rules for the h and ϕ were obtained in, for example, [11] (see also [15, 16]) in the case where SM fields do not propagate in the bulk. However, as noted earlier, preventing large FCNC and PEW corrections requires that the gauge and fermion fields propagate in the bulk. The full Feynman rules after mixing for the h and ϕ interactions with gauge bosons and fermions located in the bulk were derived in [17]. These Feynman rules are summarized in our notation in [1]. There are important modifications to the anomaly induced $\gamma\gamma$ and gg couplings as well as to the WW and ZZ couplings

For the fermions, we assume profiles such that there are no corrections to the h_0 and ϕ_0 couplings due to propagation in the bulk. This is a very good approximation for the top quark quark which must be localized near the TeV brane. Also for the bottom quark the approximation is better than 20%, see [17]. Even though the approximation is not necessarily good for light quarks, it is only the heavy quarks that impact the phenomenology of the Higgs-radion system.

In fact, the LHC Higgs-like excesses provide substantial motivation for considering a Higgs-radion RS model. The reasons are as follows. First, the most prominent excesses are in the vicinity of 125 GeV. This is an "awkward" mass for both a SM Higgs boson, in that for this mass the SM cannot be valid all the way up to m_{Pl} , and for supersymmetric models, in that fine-tuning is substantial for the large squark masses needed to achieve such a high mass, especially in the minimal supersymmetric model (MSSM). Further, the LHC excesses at 125 GeV in the $\gamma\gamma$ (and perhaps also the $ZZ \rightarrow 4\ell$ channel) appear to be larger than predicted for a SM Higgs boson. If confirmed, this, of course, rules out the SM and is also rather awkward for supersymmetric models with universal or sem-universal GUT scale boundary conditions. In contrast, excesses larger than SM expectations are natural in the context of the Higgs-radion RS model. This is because of the anomalous couplings of the radion to two gluons and to two photons that can, in particular, combine to give values larger than one for the ratios

$$R_h(X) \equiv \frac{\Gamma_h(gg)\text{BR}(h \rightarrow X)}{\Gamma_{h_{SM}}(gg)\text{BR}(h_{SM} \rightarrow X)}, \quad \text{and/or} \quad R_\phi(X) \equiv \frac{\Gamma_\phi(gg)\text{BR}(\phi \rightarrow X)}{\Gamma_{h_{SM}}(gg)\text{BR}(h_{SM} \rightarrow X)}, \quad (2)$$

where numerator and denominator are computed for the same mass, for $X = \gamma\gamma$ and $X = 4\ell$ for the h and ϕ mass eigenstates. (We note that the production of the h and ϕ are dominated by $gg \rightarrow h, \phi$ at the LHC.) Finally, the CMS data shows Higgs-like excesses not only at 125 GeV, but also at other masses, most notably at ~ 120 GeV in the 4ℓ channel and at 137 GeV in the $\gamma\gamma$ channel. Obviously, this requires more

than one Higgs-like state. If confirmed, this would rule out the SM. And, supersymmetric model parameter choices with $R(X)$ values larger than one at *two* masses have not yet been found. In the Higgs-radion RS model, it is quite easy to obtain $R(X) > 1$ at two masses and even more Higgs-like excesses can in principle be accommodated by expanding the Higgs sector of the model.

We have concentrated on the situations where either just the ~ 125 GeV excesses survive (with $R(\gamma\gamma) > 1$) or, in addition, there is a 4ℓ excess at ~ 120 GeV or a $\gamma\gamma$ excess at 137 GeV. It is particularly easy to obtain an approximate fit to the $\gamma\gamma$ excess at 125 GeV alone or to the $\gamma\gamma$ excesses at both 125 GeV and 137 GeV since it is most typically the case that $R(\gamma\gamma) > R(4\ell)$ at *both* the physical Higgs and the physical radion masses. However, there is a choice of parameters in the model where Λ_ϕ and m_0/m_{Pl} can be set independently of m_1^g for which at 120 GeV there is an excess in 4ℓ but no excess in $\gamma\gamma$ while at the same time there are both $\gamma\gamma$ and 4ℓ excesses at 125 GeV.

Finally, we note that in the most general model it is necessary to consider KK excitations in the loops responsible for the gg and $\gamma\gamma$ couplings of the unmixed h^0 . However, these contributions are only large if the "Y₂" and "Y₁" 5D quark Yukawa couplings are comparable. If $|Y_2| \ll |Y_1|$, a limit in which FCNC problems are minimal, these KK excitation corrections are quite small. (For more details, see [1].) Our results assume that this limit applies.

2 LHC Excesses

Our focus will be on the excesses seen in the $\gamma\gamma$ and 4ℓ final states that have excellent mass resolution. As already noted, in the context of the Higgs-radion model with just a single h_0 at most signals at two different masses can be described. We will consider three cases, labelled as ATLAS, CMSA and CMSB. We quantify the excesses in terms of the best fit value for $R(X) \equiv \sigma(X)/\sigma_{SM}(X)$ for a given final state X . Errors quoted for the excesses are those for $\pm 1\sigma$. The mass locations and excesses in the $\gamma\gamma$ and 4ℓ channels in these three cases are taken from Figs. 8a and 8b of [18] in the ATLAS case and from the appropriate windows of Fig. 14 of [19] in the case of CMSA and CMSB.

Table 1: Three scenarios for LHC excesses in the $\gamma\gamma$ and 4ℓ final states.

	125 GeV (ATLAS) or 124 GeV (CMS)	120 GeV	137 GeV
ATLAS	$R(\gamma\gamma) \sim 2.0^{+0.8}_{-0.8}$ $R(4\ell) \sim 1.5^{+1.5}_{-1.0}$	no excesses	no excesses
CMSA	$R(\gamma\gamma) \sim 1.7^{+0.8}_{-0.7}$ $R(4\ell) \sim 0.5^{+1.1}_{-0.7}$	$R(4\ell) \sim 2.0^{+1.5}_{-1.0}$ $R(\gamma\gamma) < 0.5$	no excesses
CMSB	$R(\gamma\gamma) \sim 1.7^{+0.8}_{-0.7}$ $R(4\ell) \sim 0.5^{+1.1}_{-0.7}$	no excesses	$R(\gamma\gamma) \sim 1.5^{+0.8}_{-0.8}$ $R(4\ell) < 0.2$

As discussed above, it is appropriate to consider two different kinds of models: one in which Λ_ϕ , m_0/m_{Pl} and m_1^g are tied together as given in Eq. (1) and there is strong lower bound on the masses of the first excitations of the gauge bosons; and one in which there is no such tie and it is appropriate to consider phenomenology for a given fixed Λ_ϕ with varying m_0/m_{Pl} . We consider these two alternatives in turn.

2.1 Lower bound on m_1^g

In this section, we consider a model along the lines of [12] in which FCNC and PEW constraints are satisfied by virtue of the fermionic profiles being peaked fairly close to the Planck brane leading to fairly definitive couplings of the fermions to the excited gauge bosons. As described earlier, a lower bound of $m_1^g \sim 1.5$ TeV can be obtained from LHC data while FCNC and PEW constraints suggest a still higher bound of ~ 3 TeV. We will show some results for both choices as we step through various possible mass locations for the Higgs and radion that are motivated by the LHC excesses in the $\gamma\gamma$ and/or 4ℓ channels. In what follows, each plot will be labelled by the value of m_0/m_{Pl} chosen and the corresponding $m_{Pl}\Omega_0$ value as calculated for the fixed m_1^g using Eq. (1).

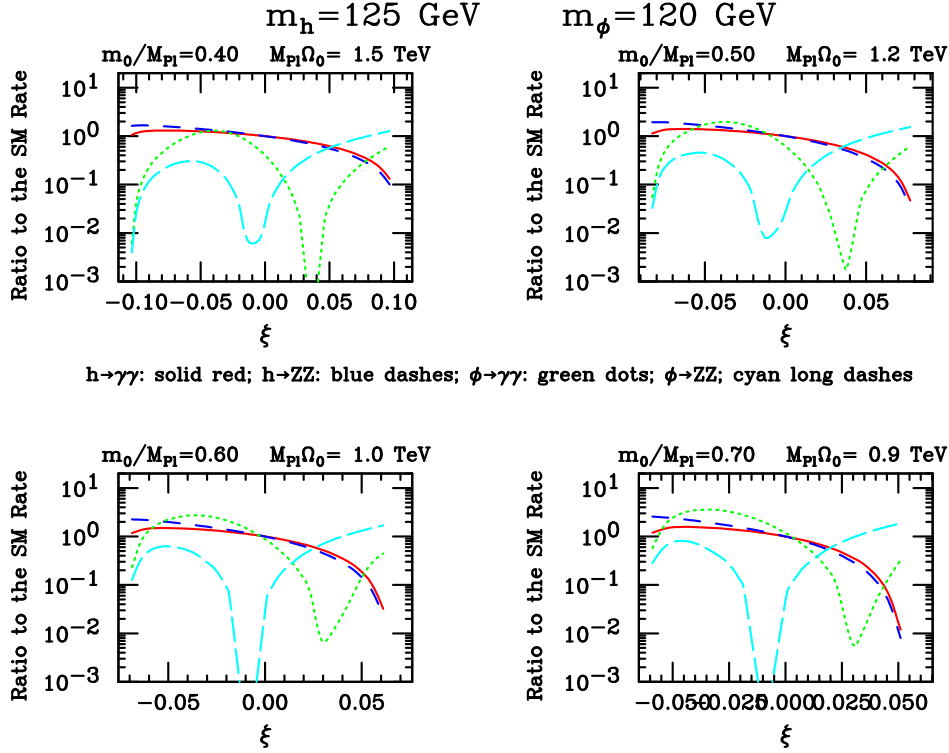


Figure 1: For $m_h = 125$ GeV and $m_\phi = 120$ GeV, we plot $R_h(X)$ and $R_\phi(X)$ for $X = \gamma\gamma$ and $X = ZZ$ (equivalent to $X = 4\ell$) as a function of ξ , assuming $m_1^g = 1.5$ TeV.

2.1.1 Signal at only 125 GeV

In Fig. 1 we illustrate some possibilities for $m_h = 125$ GeV and $m_\phi = 120$ GeV taking $m_1^g = 1.5$ TeV. First, we note that to get an enhanced $\gamma\gamma$ rate at 125 GeV, it is necessary to have $m_0/m_{Pl} \gtrsim 0.4$ and $\xi < 0$. In order to have small $R_\phi(\gamma\gamma)$ and $R_\phi(4\ell)$ at 120 GeV while at the same time $R_h(\gamma\gamma) \gtrsim 1.5$ at 125 GeV, for consistency with the ATLAS scenario, then $m_0/m_{Pl} = 0.4$ and $\xi \sim -0.09$ are good choices. The somewhat larger associated value of $R_h(4\ell)$ is still consistent within errors with the ATLAS observation at 125 GeV. We note that for the reversed assignments of $m_h = 120$ GeV and $m_\phi = 125$ GeV, we cannot find parameter choices that yield a decent description of the ATLAS 125 GeV excesses with $R_h(\gamma\gamma)$ and $R_h(4\ell)$ being sufficiently suppressed at 120 GeV.

2.1.2 Signals at 125 GeV and 120 GeV

Fig. 1 also exemplifies the fact that with $m_1^g = 1.5$ TeV the Higgs-radion model is unable to describe the CMSA scenario. In the regions of ξ for which appropriate signals are present at 125 GeV from the h , then at 120 GeV the 4ℓ and $\gamma\gamma$ rates are either both suppressed or $R_\phi(\gamma\gamma) > R_\phi(4\ell)$. This phenomenon persists at higher m_0/m_{Pl} values as well as higher m_1^g .

2.1.3 Signals at 125 GeV and 137 GeV

Let us next consider the CMSB scenario, *i.e.* neglecting the 4ℓ excess at 120 GeV in the CMS data. In Fig. 2 we see that the choices $m_0/m_{Pl} = 0.5$ and $\xi = 0.12$ give $R_h(\gamma\gamma) \sim 1.3$ and $R_h(4\ell) \sim 1.5$ at 125 GeV and

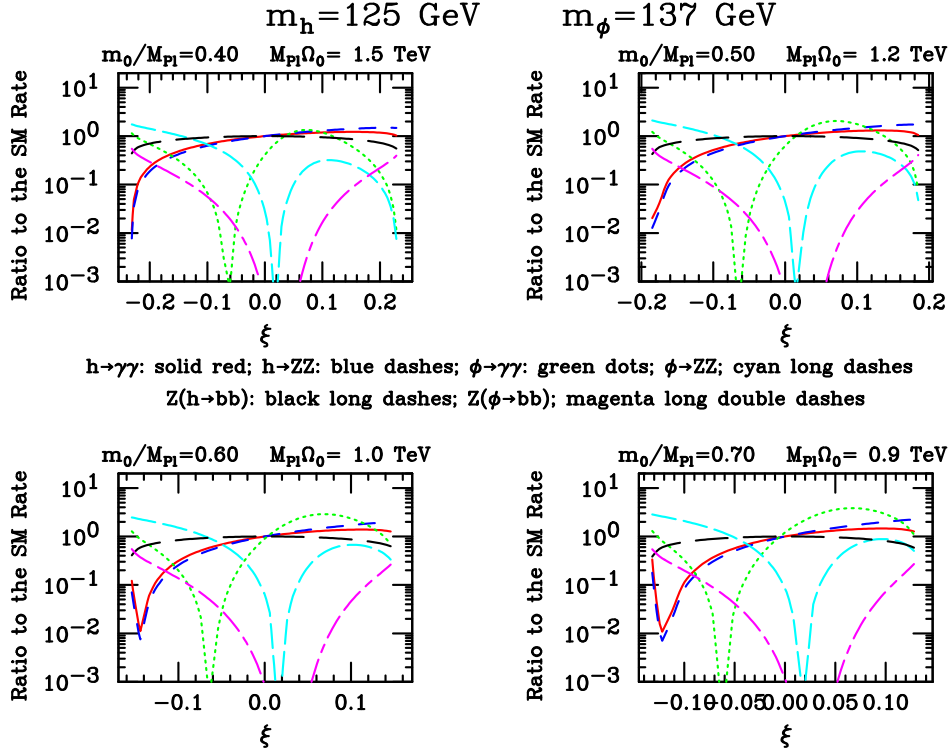


Figure 2: For $m_h = 125$ GeV and $m_\phi = 137$ GeV, we plot $R_h(X)$ and $R_\phi(X)$ for $X = \gamma\gamma$ and $X = ZZ$ (equivalent to $X = 4\ell$) as a function of ξ , assuming $m_1^g = 1.5$ TeV. Also shown are the similarly defined ratios for $Z + h$ production with $h \rightarrow b\bar{b}$ and $Z + \phi$ production with $\phi \rightarrow b\bar{b}$.

$R_\phi(\gamma\gamma) \sim 1.3$ at 137 GeV, fairly consistent with the CMSB observations. However, $R_\phi(4\ell) \sim 0.5$ at 137 GeV is a bit too large. Also shown in the figure are the rates for $Z, W + h$ with $h \rightarrow b\bar{b}$ and $Z, W + \phi$ with $\phi \rightarrow b\bar{b}$ relative to their SM counterparts. For the above $m_0/m_{Pl} = 0.5$, $\xi = 0.12$ choices, the $Z, W + h(\rightarrow b\bar{b})$ rate at 125 GeV is only slightly below the SM value, whereas the $Z, W + \phi(\rightarrow b\bar{b})$ rate is about 10% of the SM level predicted at 137 GeV. The former is consistent with the poorly measured $b\bar{b}$ rate at 124 GeV while confirmation of the latter would require much more integrated luminosity.

We also note that it is not possible to get enhanced $\gamma\gamma$ and 4ℓ h signals at 125 GeV without having visible 137 GeV ϕ signals, *i.e.* the ATLAS scenario of no observable excesses other than those at 125 GeV cannot be realized for $m_\phi = 137$ GeV.

For this case, it is also interesting to consider results for $m_h = 125$ GeV and $m_\phi = 137$ GeV for the higher value of $m_1^g = 3$ TeV. One finds that $R_h(\gamma\gamma)$ and $R_h(4\ell)$ are both $\lesssim 1$ (or less) except for $m_0/m_{Pl} = 0.7$ and large ξ for which $R_\phi(\gamma\gamma) \ll 1$. Thus, a reasonable description of the CMSB scenario requires relatively small m_1^g .

2.1.4 Signals at 125 GeV and high mass

A general question is whether one could explain the ATLAS 125 GeV excesses as being due to the h or ϕ with the other being at high mass. If $m_h = 125$ GeV and $m_\phi > 500$ GeV, one finds that $R_h(\gamma\gamma) \sim R_h(4\ell) \sim 1$ for ξ above some minimum (negative) value, with values substantially below 1 for more negative ξ . In any case, precision electroweak constraints are violated if $|\xi|$ is not quite modest in size since at large $|\xi|$ the

ϕVV ($V = W, Z$) couplings become of SM strength or larger. For more discussion see [20].

If the mass assignments are reversed, $m_\phi = 125$ GeV and $m_h > 500$ GeV, then at the most positive ξ values one can achieve $R_\phi(\gamma\gamma) \sim 2$ and $R_\phi(4\ell) \sim 1$ at 125 GeV for $m_0/m_{Pl} = 0.4$ and 0.5. However, this scenario is even less consistent with precision electroweak constraints since for all ξ the h alone has hVV couplings that are at least SM-like. Much larger Λ_ϕ would be needed to have a hope of achieving PEW consistency [20] and for large Λ_ϕ ATLAS-like $>SM$ signals at $m_h = 125$ GeV would not be achievable. In addition, the $h \rightarrow 4\ell$ signal at high mass would be at least as large as predicted for a high-mass SM-like Higgs and therefore quite observable if $m_h \lesssim 500$ GeV, as seemingly inconsistent with ATLAS and CMS data. If $m_h \sim 1$ TeV, then the 4ℓ signal would be beyond current LHC reach but PEW inconsistency would be much worse. Thus, we conclude that for the Higgs-radion model to be of interest, both m_h and m_ϕ should be modest in size.

2.2 Fixed Λ_ϕ

In this section, we consider the second type of model discussed in the introduction in which there is no direct tie between m_1^g , Λ_ϕ and m_0/m_{Pl} . In this case, we feel free to consider the rather low values of Λ_ϕ , $\Lambda_\phi = 1$ TeV and $\Lambda_\phi = 1.5$ TeV, for which the Higgs-radion model can yield LHC rates in the $\gamma\gamma$ and 4ℓ channels that exceed those that are predicted for a SM Higgs. We note that when the gauge bosons propagate in the bulk, the phenomenology does not depend on Λ_ϕ alone — there is strong dependence on m_0/m_{Pl} when m_0/m_{Pl} is small. However, for large $m_0/m_{Pl} \gtrsim 0.5$ the phenomenology is determined almost entirely by Λ_ϕ , but is still not the same as found in the case where all fields are on the TeV brane. Once again, we step through a few possible mass locations for the Higgs and radion that are motivated by the LHC excesses in the $\gamma\gamma$ and/or 4ℓ channels.

2.2.1 Signal only at 125 GeV

As shown in Fig. 3, the choice of $\Lambda_\phi = 1$ TeV with $m_\phi = 125$ GeV and $m_h = 120$ GeV gives a reasonable description of the ATLAS excesses at 125 GeV with no visible signals at 120 GeV in either the $\gamma\gamma$ or 4ℓ channels when one chooses $m_0/m_{Pl} = 1$ and $\xi = -0.016$. In contrast, for $\Lambda_\phi = 1.5$ TeV the 125 GeV predicted excesses are below $1 \times SM$ and thus would not provide a good description of the ATLAS data. For the reversed assignments of $m_h = 125$ GeV and $m_\phi = 120$ GeV any choice of parameters that gives a good description of the 125 GeV signals always yields a highly observable $\gamma\gamma$ signal at 120 GeV.

2.2.2 Signals at 125 GeV and 120 GeV

The closest that we can come to fitting this CMSA scenario is to take $m_h = 125$ GeV and $m_\phi = 120$ GeV. One finds that if ξ is at its maximum value and $m_0/m_{Pl} = 1.1$ then the $\gamma\gamma$ and 4ℓ signals at $m_h = 125$ GeV are low, but still within -1σ of the CMS data while at $m_\phi = 120$ GeV one finds $R_\phi(4\ell) \sim 2.5$ while $R_\phi(\gamma\gamma) \sim 0.3$, which values are roughly consistent with the CMSA situation. For the reversed assignments of $m_h = 120$ GeV and $m_\phi = 125$ GeV, Fig 3 illustrates the fact that a satisfactory description of the two CMSA excesses is not possible — for ξ such that appropriate 125 GeV excesses are present, $R_h(\gamma\gamma)$ and $R_h(4\ell)$ at 120 GeV are always small so that the 4ℓ excess at 120 GeV is not explained.

2.2.3 Signals at 125 GeV and 137 GeV

Let us now consider the CMSB scenario. For $\Lambda_\phi = 1$ TeV, one finds $m_h = 125$ GeV and $m_\phi = 137$ GeV with the choices $m_0/m_{Pl} = 0.6$ and $\xi = -0.05$ give $R_h(\gamma\gamma) \sim 2$ and $R_h(4\ell) \sim 1$ at 125 GeV, while $R_\phi(\gamma\gamma) \sim 2$ and $R_\phi(4\ell) \sim 0.4$ at 137 GeV, an ok description of the CMSB excesses. An equally rough description of this same situation is also possible for $\Lambda_\phi = 1$ TeV with $m_0/m_{Pl} = 0.8$ and $\xi = 0.05$.

For $\Lambda_\phi = 1.5$ TeV a somewhat better simultaneous description of these excesses is possible. Fig. 4 shows some results for $m_h = 125$ GeV and $m_\phi = 137$ GeV. For $m_0/m_{Pl} = 0.25$ and $\xi \sim -0.1$ one finds $R_h(\gamma\gamma) \sim 2$ and $R_h(4\ell) \sim 1.5$ at $m_h = 125$ GeV, while $R_\phi(\gamma\gamma) \sim 2$ and $R_\phi(4\ell) \ll 1$ at $m_\phi = 137$ GeV, in pretty good agreement with the CMSB scenario.

If we reverse the configuration to $m_h = 137$ GeV and $m_\phi = 125$ GeV, the only parameter choices that come close to describing the two excess are $\Lambda_\phi = 1$ TeV with $m_0/m_{Pl} = 0.8$ and $\xi \sim 0.05$ for which one finds that the $m_\phi = 125$ GeV $\gamma\gamma$ and 4ℓ signals and the $m_h = 137$ GeV $\gamma\gamma$ signal are all at the level of

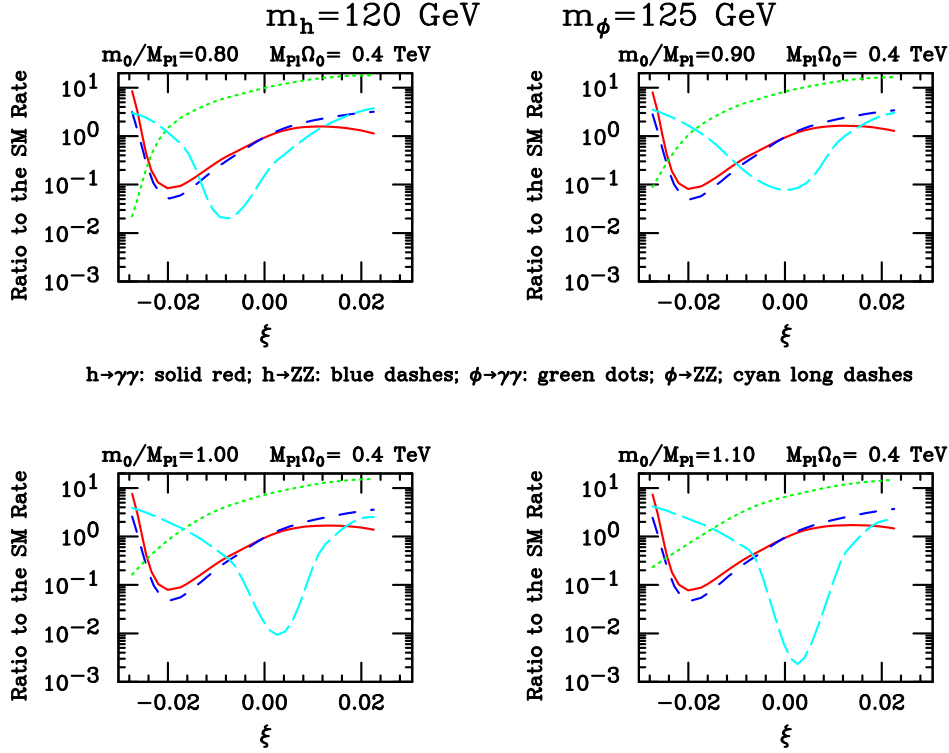


Figure 3: For $m_h = 120$ GeV and $m_\phi = 125$ GeV, we plot $R_h(X)$ and $R_\phi(X)$ for $X = \gamma\gamma$ and $X = ZZ$ (equivalent to $X = 4\ell$) as a function of ξ taking Λ_ϕ fixed at 1 TeV.

$\sim 1.4 \times \text{SM}$. However, the $m_h = 137$ GeV 4ℓ signal is at the level of $\sim 0.6 \times \text{SM}$ which is 4σ away from the CMS central value at this mass. For these mass assignments, the higher $\Lambda_\phi = 1.5$ TeV value does not provide any parameter choices that come close to describing the CMS excesses — the $m_\phi = 125$ GeV signals are never both sufficiently large *at the same time* to fit the observed signals.

2.2.4 Signals at 125 GeV and higher mass

We choose not to show any specific plots for this situation. For $\Lambda_\phi = 1$ TeV or 1.5 TeV, it is possible to choose one of either the h or ϕ to have a mass of 125 GeV and find m_0/m_{Pl} and ξ values that result in a decent description of the 125 GeV ATLAS excesses. However, these scenarios always are such as to imply a large inconsistency with PEW constraints and, if the higher mass is chosen below 500 GeV, a highly observable 4ℓ signal that would be inconsistent with ATLAS and CMS observations in that region of mass.

2.2.5 SM Higgs at 125 GeV and Signal at 137 GeV

It is still quite conceivable that, after accumulating more data, the $\gamma\gamma$ and 4ℓ excesses at ~ 125 GeV will converge to those appropriate for a SM Higgs boson. Such a situation would correspond to taking $\xi = 0$ in the Higgs-radion model. In this case, one can ask whether or not there could be a radion at some nearby mass and what its experimental signature would be. To exemplify, let us suppose that the signal at 137 GeV of the CMSB scenario survives. In Fig. 5 we plot $R_\phi(X)$ for $X = \gamma\gamma$ and $X = 4\ell$ as a function of Λ_ϕ for a selection of m_0/m_{Pl} values, taking $\xi = 0$. We also display ratios to the SM for WW fusion production of the ϕ , with

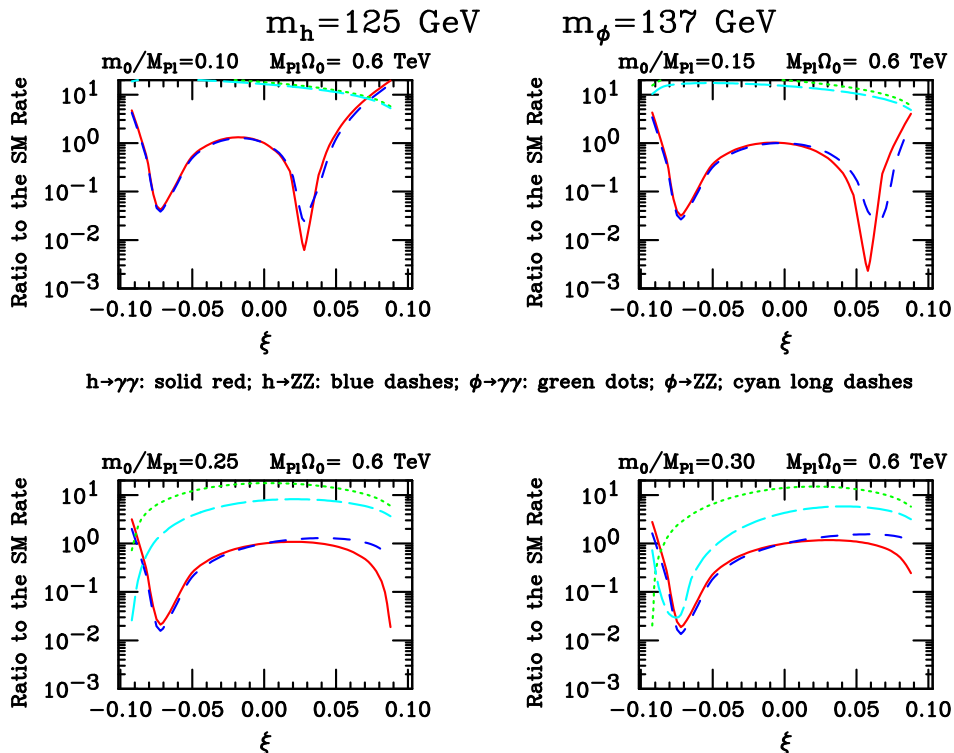


Figure 4: For $m_h = 125$ GeV and $m_\phi = 137$ GeV, we plot $R_h(X)$ and $R_\phi(X)$ for $X = \gamma\gamma$ and $X = ZZ$ (equivalent to $X = 4\ell$) as a function of ξ taking Λ_ϕ fixed at 1.5 TeV.

$\phi \rightarrow \gamma\gamma$, 4ℓ and $b\bar{b}$, as well as associated $Z\phi$ production with $\phi \rightarrow b\bar{b}$. One observes that a nice description of the $R(\gamma\gamma) \sim 2$ excess at 137 GeV is possible, for example, for $m_0/m_{Pl} = 0.3$ at $\Lambda_\phi \sim 2.8$ TeV with the 4ℓ signal (and all other signals) being very suppressed. As also apparent, other choices of m_0/m_{Pl} and Λ_ϕ will also yield $R_\phi(\gamma\gamma) \sim 2$ with varying levels of 4ℓ and $b\bar{b}$ signals. (However, to suppress $R_\phi(4\ell)$ below 0.2 while achieving $R_\phi(\gamma\gamma) \sim 2$ requires $m_0/m_{Pl} \geq 0.3$.) We also note that for $\xi = 0$ the $Z, W + \phi(\rightarrow b\bar{b})$ is greatly suppressed relative to its SM counterpart due to the very suppressed $ZZ\phi$ coupling.

Plots for the case of a SM Higgs at 125 GeV and $m_\phi = 120$ GeV look very similar and, in particular, it is not possible to find parameters for which the 4ℓ signal substantially exceeds the $\gamma\gamma$ signal — the reverse always applies, as one anticipates from the enhanced anomalous $\gamma\gamma$ coupling of the (unmixed) ϕ .

3 Summary and Conclusions

The Randall Sundrum model solution to the hierarchy problem yields interesting phenomenology for the Higgs-radion sector, especially when Higgs-radion mixing is allowed for, and can be made consistent with FCNC and PEW constraints if fermions and gauge bosons propagate in the 5th dimension. At the moment, there are interesting hints at the LHC of narrow excesses above SM backgrounds in the $\gamma\gamma$ and $ZZ \rightarrow 4\ell$ channels, as well as a broad excess in the $WW \rightarrow \ell\nu\ell\nu$ channel. ATLAS sees excesses in the $\gamma\gamma$ and 4ℓ channels at a mass of ~ 125 GeV of order $2 \times \text{SM}$ and $1.5 \times \text{SM}$ respectively. CMS sees a $\gamma\gamma$ excess of order $1.5 \times \text{SM}$ at ~ 124 GeV and constrains the 4ℓ channel at this mass to be less than $\sim 1.5 \times \text{SM}$. Additional excesses at 120 GeV (in the 4ℓ channel) and at 137 GeV (in the $\gamma\gamma$ channel) are present in the CMS data.

Here, we summarized two models with Higgs-radion mixing within the Randall Sundrum model context.

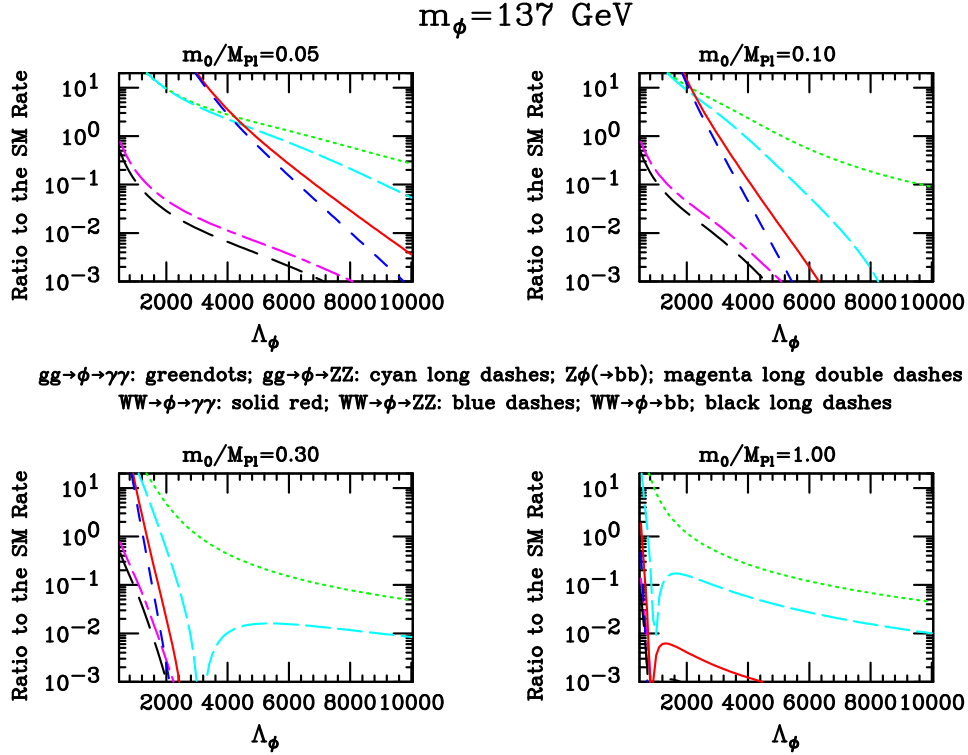


Figure 5: For $m_\phi = 137 \text{ GeV}$, we plot $R_\phi(X)$ for $X = \gamma\gamma$ and $X = ZZ$ (equivalent to $X = 4\ell$) as functions of Λ_ϕ taking $\xi = 0$. We also plot ratios to the SM for $Z \rightarrow Z\phi$ with $\phi \rightarrow b\bar{b}$ and for $WW \rightarrow \phi \rightarrow X$ for $X = \gamma\gamma, ZZ$ and $b\bar{b}$.

In the first model, the light fermion profiles are taken to be peaked near the Planck brane in order to avoid corrections to FCNC and PEW constraints that are too large. In this case, there is a lower bound on the mass of the 1st excited gluon state of order $m_1^g \geq 1.5 \text{ TeV}$ and it is necessary to correlate Λ_ϕ (the radion field vacuum expectation value) with the curvature ratio m_0/m_{Pl} and the m_1^g lower bound appropriately. In the second model considered there is no strong tie between the above parameters and it is most appropriate to consider fixed Λ_ϕ values while varying m_0/m_{Pl} — we studied the phenomenologically interesting choices of $\Lambda_\phi = 1 \text{ TeV}$ and 1.5 TeV .

Since the single Higgs plus radion model can describe at most two Higgs-like excesses, we considered three scenarios labelled as: ATLAS, with $\gamma\gamma$ and 4ℓ excesses at 125 GeV larger than SM and no other significant excesses; CMSA, with $\gamma\gamma$ and 4ℓ excesses at 124 GeV (the $\gamma\gamma$ excess being above SM level) and a 4ℓ excess at 120 GeV ; and, CMSB, with a $\gamma\gamma$ and 4ℓ excesses at 124 GeV along with a $\gamma\gamma$ excess at 137 GeV larger than would have been predicted for $m_{h_{SM}} = 137 \text{ GeV}$. In both the fixed m_1^g and the fixed Λ_ϕ model possibilities, the signal levels of the ATLAS and CMSB scenarios could be nicely described. Only for the 2nd model class could a (marginally) satisfactory description of the CMSA case be found. In general, successful fitting of the ATLAS and CMSB excesses required a modest value for the radion vacuum expectation value, typically $\Lambda_\phi \lesssim 2 \text{ TeV}$, and mostly $m_0/m_{Pl} \gtrsim 0.5$, a range that the most recent discussion suggests is still consistent with higher curvature corrections to the RS scenario being small.

We also considered expectations for the radion signal in the case where the Higgs signal was assumed to ultimately converge to precisely that for a SM Higgs of mass 125 GeV . This situation would arise if there is no Higgs-radion mixing. We found that interesting excesses at the radion mass would be present for low enough Λ_ϕ , namely $\Lambda_\phi \lesssim 3 \text{ TeV}$, but would always be characterized by a $\gamma\gamma$ signal that substantially exceeds the 4ℓ signal (as appropriate for the CMS excesses at 137 GeV but in definite contradiction with the CMS excesses at 120 GeV).

Acknowledgments

Thanks go to Kaustubh Agashe, Felix Brummer, Csaba Csaki, Gero Von Gersdorff, Tom Rizzo and John Terning for illuminating discussions on radion physics. JFG thanks his collaborators on this project, Bohdan Grzadkowski and Manuel Toharia. JFG is supported by US DOE grant DE-FG03-91ER40674.

References

- [1] B. Grzadkowski, J. F. Gunion, and M. Toharia, arXiv:1202.5017 [hep-ph].
- [2] L. Randall and R. Sundrum, Phys. Rev. Lett. **83** (1999) 3370 [arXiv:hep-ph/9905221];
- [3] H. Davoudiasl, J. L. Hewett and T. G. Rizzo, Phys. Lett. B **473**, 43 (2000) [hep-ph/9911262].
- [4] A. Pomarol, Phys. Lett. B **486**, 153 (2000) [hep-ph/9911294].
- [5] T. Gherghetta, A. Pomarol, Nucl. Phys. **B586**, 141-162 (2000). [hep-ph/0003129].
- [6] H. Davoudiasl, J. L. Hewett, T. G. Rizzo, Phys. Rev. **D63**, 075004 (2001). [hep-ph/0006041].
- [7] C. Csaki, J. Erlich and J. Terning, Phys. Rev. D **66**, 064021 (2002) [hep-ph/0203034].
- [8] J. L. Hewett, F. J. Petriello and T. G. Rizzo, JHEP **0209**, 030 (2002) [hep-ph/0203091].
- [9] K. Agashe, A. Delgado, M. J. May and R. Sundrum, JHEP **0308**, 050 (2003) [hep-ph/0308036].
- [10] K. Agashe, H. Davoudiasl, G. Perez and A. Soni, Phys. Rev. D **76**, 036006 (2007) [hep-ph/0701186].
- [11] D. Dominici, B. Grzadkowski, J. F. Gunion and M. Toharia, Nucl. Phys. B **671**, 243 (2003) [arXiv:hep-ph/0206192]; Acta Phys. Polon. B **33**, 2507 (2002) [arXiv:hep-ph/0206197].
- [12] K. Agashe, A. Belyaev, T. Krupovnickas, G. Perez and J. Virzi, Phys. Rev. D **77**, 015003 (2008) [hep-ph/0612015].
- [13] S. Rappoccio [CMS Collaboration], arXiv:1110.1055 [hep-ex].
- [14] The ATLAS Collaboration, ATLAS-CONF-2011-123.
- [15] G. F. Giudice, R. Rattazzi and J. D. Wells, Nucl. Phys. B **595**, 250 (2001) [arXiv:hep-ph/0002178].
- [16] J. L. Hewett and T. G. Rizzo, JHEP **0308**, 028 (2003) [hep-ph/0202155].
- [17] C. Csaki, J. Hubisz, S. J. Lee, Phys. Rev. **D76**, 125015 (2007). [arXiv:0705.3844 [hep-ph]].
- [18] ATLAS Collaboration, <http://cdsweb.cern.ch/record/1406358ATLAS-CONF-2011-163>.
- [19] CMS Collaboration, <http://cdsweb.cern.ch/record/1406347/CMS-PAS-HIG-11-032>.
- [20] J. F. Gunion, M. Toharia and J. D. Wells, Phys. Lett. B **585**, 295 (2004) [hep-ph/0311219].